Journal of Groundwater Science and Engineering
ISSN 2305-7068
Indexed by ESCI CABI CSA Scopus GeoRef AJ CNKI

Determination of groundwater potential distribution in Kulfo-Hare watershed through integration of GIS, remote sensing, and AHP in Southern Ethiopia

Edmealem Temesgen, Demelash Wendmagegnehu Goshime, Destaw Akili

Citation:
Temesgen E, Goshime DW, Akili D. 2023. Determination of groundwater potential distribution in Kulfo-Hare watershed through integration of GIS, remote sensing, and AHP in Southern Ethiopia. Journal of Groundwater Science and Engineering, 11(3): 249-262.

View online: https://doi.org/10.26599/JGSE.2023.9280021

Journal homepage: http://gwse.iheg.org.cn

Research Paper

Determination of groundwater potential distribution in Kulfo-Hare watershed through integration of GIS, remote sensing, and AHP in Southern Ethiopia

Edmealem Temesgen[1*], Demelash Wendmagegnehu Goshime[1], Destaw Akili[1]

[1] *Water Resources and Irrigation Engineering, Arba Minch Water Technology Institute, Arba Minch University, Arba Minch, Ethiopia.*

Abstract: Identification of groundwater potential areas (GPA) is important in regions facing surface water scarcity, as it assists in effective planning and utilization of groundwater for various purposes. This study employs the methods of remote sensing (RS), geographic information system (GIS) model, and analytical hierarchy process (AHP), multi-criteria decision analysis (MCDA) to locate and map the prospective groundwater areas in the Kulfo-Hare watershed. Seven significant groundwater influencing factors were selected for the determination of groundwater potential in the area: Geology, land use/land cover (LULC), soil, rainfall, slope, drainage density, and lineament density. By applying a five-class classification scheme (very low, low, moderate, high, and very high), the GIS models were used to define the distribution of groundwater potential areas in terms of area coverage (km^2), percentage and mapping. The results show that the groundwater potential (GWP) distribution in the research region is as follows: 9.7% (6 035.9 ha) classified as very high GWP, 29.6% (18 606 ha) classified as high, 24.5% (15 245 ha) classified as moderate, 18.1% (11 431 ha) as low and 18.1% (11 492 ha) very low GWP, on the basis of the weighted overlay evaluation. Although a few regions are identifies as extremely low GWP, most of the study area is characterized by very high to moderate GWP. These findings provide valuable insight for sustainable groundwater planning by the government bodies, decision-makers, and private sectors.

Keywords: Groundwater potential zone; Multi-criteria decision; Pairwise; Normalization; Weighed overlay analysis

Received: 25 Dec 2022/ Accepted: 12 Jul 2023/ Published: 15 Sep 2023

Introduction

Groundwater is recognized as primary freshwater source that meets the demands for water in various sectors such as agricultural, residential, industrial, and others (Agarwal et al. 2013; Biswas et al. 2013; Das and Mukhopadhyay, 2018). However, the availability of groundwater often falls short of societal needs (Mukherjee et al. 2012). Poor water resource management and unscientific utilization exacerbate this issue, particularly in developing countries where the demand for water resources is rapidly increasing (Thapa et al. 2017; Holden, 2014). Therefore, it is necessary to develop a sustainable groundwater management plan to accurately utilize the important resources, which requires the delineation of groundwater potential areas using geospatial technologies.

Geospatial technologies such as GIS and remote sensing have become essential tools in water studies due to their capability to generate spatio-temporal information and perform spatial data analysis and prediction (Magesh et al. 2012). These technologies are particularly applicable in identifying and demarcating groundwater potential

*Corresponding author: Edmealem Temesgen, *E-mail address*: danicho1255@gmail.com

DOI: 10.26599/JGSE.2023.9280021

Temesgen E, Goshime DW, Akili D. 2023. Determination of groundwater potential distribution in Kulfo-Hare watershed through integration of GIS, remote sensing, and AHP in Southern Ethiopia. Journal of Groundwater Science and Engineering, 11(3): 249-262.

zones using multi-criteria decision-making analysis (MCDA) (Ramamoorthy and Rammohan, 2015). The MCDA combines qualitative and quantitative approaches (Saaty and Vargas, 2012). Remote sensing not only provides a wide- scale distribution of observations in both time and space, saving time and resources.

In Ethiopia, several scholars have used GIS software and remote sensing methods to investigate groundwater potential and analyze the groundwater within the potential zones. Studies conducted in the Middle Awash River basins (Bashe, 2017) and the Bilate River Catchment in Ethiopia's Southern Rift Valley (Gintamo, 2014) are a few examples addressing the country's water resource capacity. However, the groundwater potential of the Kulfo-Hare watershe, despite its geological, geophysical, and hydrogeological significance, has not been adequately explored. Thus, using GIS software and remote sensing methods, and AHP approaches can help bridge the information and knowledge gap by assessing the groundwater potential of research area.

The Kulfo-Hare watershed is one of the sources of water for the Abaya-Chamo basin, located on the northern escarpment of the Rift Valley in Ethiopia. Despite significant potential for agricultural land and groundwater resources, the basin is predominantly inhabited by an agrarian community heavily reliant on rain-fed agriculture. However, the region faces critical water scarcity for domestic consumption. Therefore, exploring the groundwater potential areas is essential for discovering and developing water resources in the research region for home usage, irrigation, drinking, and industrial purposes.

The aim of this study is to assess the groundwater potential zones in the Kulfo-Hare watershed using GIS and remote sensing, and AHP methods. The study incorporates various factors that influence groundwater potential. These factors include lineament density, geology formation, drainage density, rainfall, slope, soil, and land use/land cover (LULC).

In this study, AHP algorithm and weight overlay analysis are employed to construct the groundwater potential zones (Bashe, 2017). Weighted overlay analysis is a model system that combines the geometry and attributes of all thematic layers in a GIS environment to create a composite map (Mussa et al. 2020). It is a multi-parametric technique that allows users to integrate multiple raster layers to obtain the final result. The objective of the weighted overlay analysis is to generate to generate a comprehensive model that reflects the potential of groundwater resources in a given location based on the analysis of selected factors and their associated weights.

These approaches offer quick, accurate, and cost-effective approaches for generating valuable data on geological and geomorphological factors that facilitate the demarcation of groundwater potential areas (Elewa and Qaddah, 2010; Samy et al. 2012; Samy and Mohamed, 2013). Therefore, the primary objective of this study is to determine groundwater potential areas as percentage and map using topography, hydrological and geological factors, along with a multi-criteria approach.

1 Study area

1.1 Location

The study area, the Kulfo-Hare catchment, is a sub-catchment of the Abaya-Chamo sub-Basin in the Rift Valley. It is located between the longitude of 37°19'00"–37°36'00"E, latitude 5°54'30"–6°11'30" N, at an altitude of 1 203 m above main sea level and 454 km south of Addis Ababa. The total area of Kulfo-Hare River basin is 622.69 km^2 (Fig. 1).

1.2 Climate

The analysis of thirty-two year data spanning from 1987 to 2022 reveals that the average minimum and maximum temperature of Arba Minch are 17.40°C (December) and 30.63°C (March), respectively. The rainfall pattern at Arba Minch station follows a bi-modal distribution, with one peak season from April to June and another from September to October. The average annual precipitation in the area is 885.22 mm as shown in Fig. 2. The source of irrigation water used in the study area is from Kulfo and Hare Rivers which ultimately discharge into Lake Abaya and Lake Chamo.

1.3 Geological formation, soil type and land use /cover

The Kulfo-Hare catchment is characterized by Tertiary and Quaternary volcanism, with the volcanic rocks of Oligocene to Middle Miocene ages located in the research area. The volcanic rocks are primarily found in the highlands and a lesser extent on the rift floor (Corti et al. 2013). They consist of interstratified ignimbrite beds and basaltic lava flows, overlain by extensive rhyolites, tuffs, and

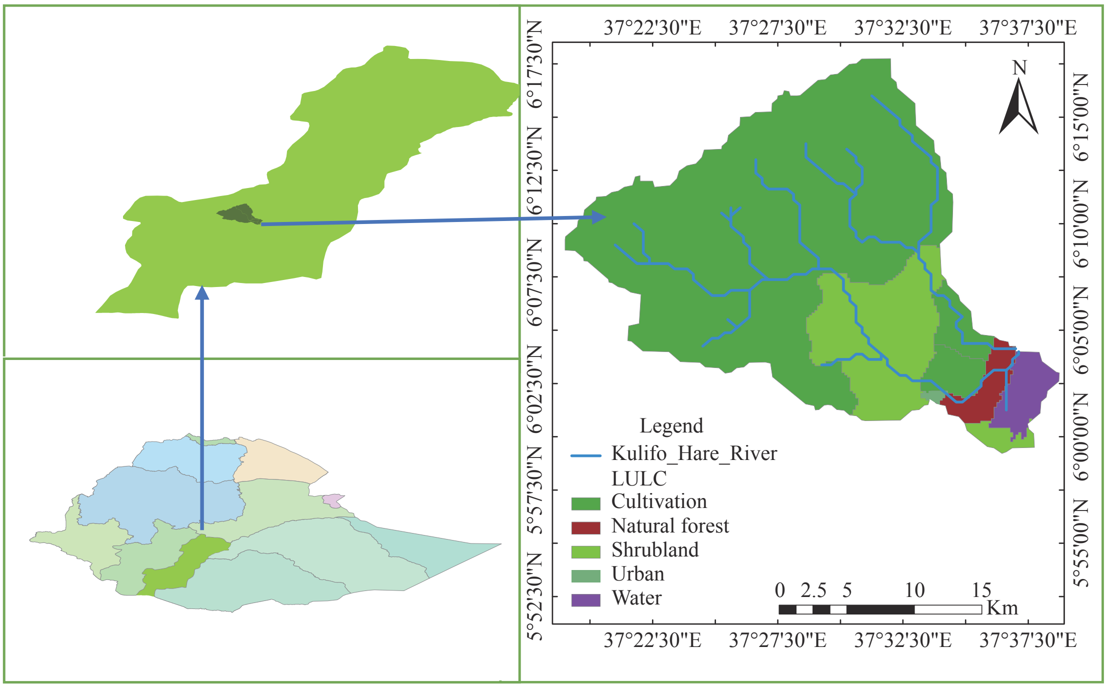

Fig. 1 Location map of the study area

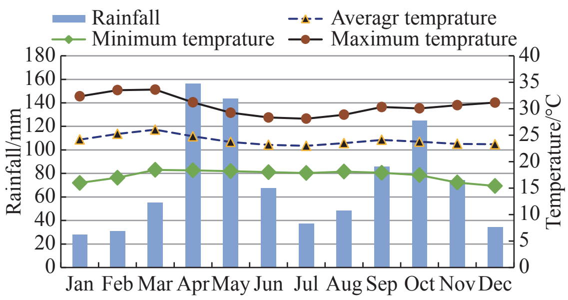

Fig. 2 The rainfall and temperature pattern of the study area

basalts. The dominant rock type is basalt, which is highly jointed and weathered, mainly exposed in the Chencha highlands (Ebinger et al. 1993).

In respect of soil type, The Kulfo-Hare catchment can be classified by four main categories: Cambisols, ferralsols, regosols, and fluvisols (FAO, 1998). The catchment is predominantly used for agriculture, with the flat alluvial land surrounding the river being extensively utilized for this purpose. The land cover in the catchment consists of thick bushlands, open woodlands, forests, and grasslands, cultivated areas (Ashebir et al. 2018).

2 Materials and methods

2.1 Data source and preparation of thematic layers

To assess the potential groundwater regions in the Kulfo-Hare watershed, seven factors were selected: Geology, LULC, soil, rainfall, slope, drainage density, and lineament density. These layers were processed and generated using GIS, incorporating the data derived from field work and remote sensing satellite imagery. Prior to analysis, all selected thematic layers were rasterized and projected into UTM Zone 37 WGS 84, with a spatial resolution of 30 m. Table 1 provides a summary of the data sources and their respective details.

2.2 Method

Data on groundwater potential variables were obtained from remote sensing satellites, as detailed in Table 1. GIS pre-processing techniques were employed to convert the data from vector to raster formats. Following the conversion, reclassification of the rasterized thematic layers was conducted using a constant cell size. The values of weight factors were then applied to the MCDA-AHP model, thereby the final groundwater potential map for the Kulfo-Hare catchment was generated by calculating all of the raster layers in the GIS environment. The flow diagram illustrating the conceptual framework and methodology of the study is presented in Fig. 3.

2.3 Weight factor and groundwater potential zoning

The Analytical Hierarchy Process (AHP), estab-

Table 1 Groundwater potential estimation factors and their sources

Factors	Data source	Data details	Source reference
Slope	ASTER GDEM	Version 3, (30 × 30) m	https://search.earthdata.nasa.gov
Drainage density	ASTER GDEM	Version 3, (30 × 30) m	https://search.earthdata.nasa.gov
Geology	Geological survey ASTER	Data vector layer: 11 091 958	https://search.earthdata.nasa.gov
Lineament density	Geological survey ASTER	Data vector layer: 11 091 958	https://search.earthdata.nasa.gov
Land use/land cover	USGS	Landsat 8 (30 × 30) m	https://earthexplorer.usgs.gov
Soil	FAO	Digital soil map of the World	http://www.fao.org
Rainfall	CRUTS v. 4.04	High-resolution gridded data, 0.5°×0.5°	https://sites.uea.ac.uk/cru/da

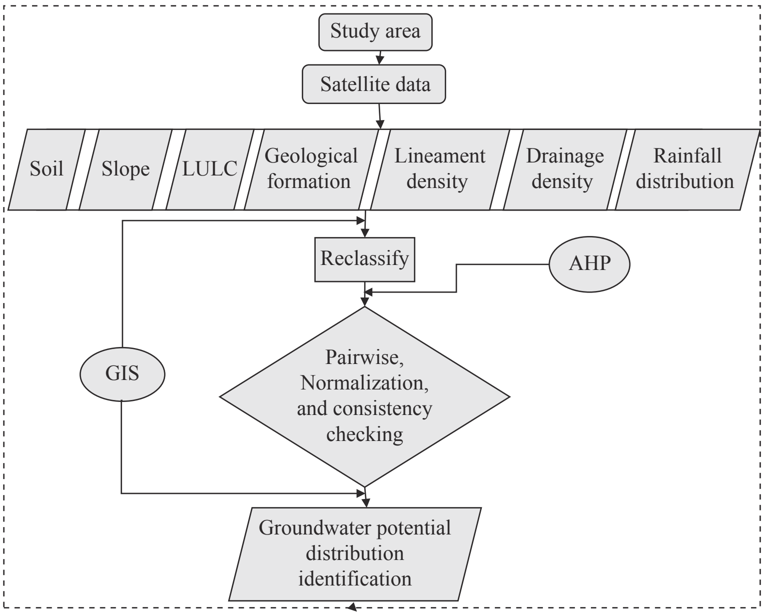

Fig. 3 Flowchart presenting methodology of the study

lished by Saaty (1999), was employed as an appropriate decision-making approach based on multiple criteria. AHP enables the hierarchical structuring of a set of parameters by assigning weights to each criterion, thereby reducing decision-making complexity (Pramanik, 2016). According to Sener et al. (2011), AHP is a systematic and reliable technique for decision-making that utilizes expert views and GIS analysis to assess multiple variables.

The weights assigned of each parameter and their normalization are critical as they significantly influence the final outcomes (Muralitharan and Palanivel, 2015). Although various methods exist for weight estimation, AHP is considered a favorable technique in groundwater modeling due to its ability to provide rapid, reliable, and cost-effective results (Murmu et al. 2019). The AHP process consists of four steps: Weighting, pairwise comparison matrix, weight normalization, and consistency check (Benjmel et al. 2020; Ghosh et al. 2020).

In the study, a total of seven parameters were selected to assess the flow factor and storage capacity of groundwater in the region. The weights for each parameter were assigned based on expert judgment, field expertise, and extensive literature survey (Agarwal and Garg, 2016; Yeh et al. 2010; Saha, 2017; Singh et al. 2018; Andualem and Demeke, 2019; Abijith et al. 2020; Arefin, 2020; Ghosh et al. 2020; Tolche, 2020). Higher weights indicate greater impact, while lower weights correspond to a minimal influence on groundwater potential. The weights of each criterion were assigned using Saaty's scale of relative importance, ranging from 1 to 9, to compare all characteristics of the thematic layers in a matrix format. This comparison is essential for calculating measurements. Saaty's scale assigns a value of '9' to indicate "great importance" and a value of '1' to indicate "equal importance" (Table 2).

The weights derived from the pairwise comparison matrix were then used for the normalizing process using the principal vector technique described by Saaty (Agarwal and Garg, 2016; Ghosh et al. 2020). After normalization, the

Table 2 Importance scale (1-9) and random consistency index (RI) (Saaty, 1999)

Intensity	**1**	**2**	**3**	**4**	**5**	**6**	**7**	**8**	**9**
Definition	Equal	Weak	Moderate	Moderate plus	Strong	Strong plus	Very strong	Very very strong	Extreme
RI value	0	0	0.58	0.9	1.12	1.24	1.32	1.41	1.45

consistency index (*CI*), and consistency ratio (*CR*) were calculated to assess the consistency of the pairwise matrix. The four phases of AHP were computed using the following procedures (Arefin, 2020).

Step 1: Pairwise comparison matrix (PCM) was determined using Equation (1):

$$X = \begin{bmatrix} X_{11}X_{12}\cdots X_{1n} \\ X_{21}X_{22}\cdots X_{2n} \\ \cdots\cdots\cdots\cdots \\ \cdots\cdots\cdots\cdots \\ X_{n1}X_{n1}\cdots X_{nn} \end{bmatrix} \quad (1)$$

Where: X is the Pairwise comparison matrix, and X_{nn} is the indicator of the pairwise matrix element.

Step 2: Normalizing of weights using Equation (2):

$$NW = \left(\frac{GM}{\sum_{n=1}^{N} GM_n} \right) \quad (2)$$

Where: NW is normalized weights, GM_n is the geometric mean of n^{th} row of the pairwise matrix (X).

Further, GM_n can be expressed using Equation (3):

$$GM_n = \sqrt[n]{X_{1n} * X_{2n} \cdots\cdots\cdots X_n * N} \quad (3)$$

Step 3: The consistency ratio (*CR*) was used to validate the pairwise judgment matrix which was calculated by using Equation (4)

$$CR = \frac{CI}{RI} \quad (4)$$

Where: *CI* is the Consistency index, *RI* is the random index.

According to Saaty (1999), a *CR* value of 0.10 is sufficient to proceed with the assessment. If the *CR* value is greater than 0.10, the analysis needs to be revised from the beginning to identify the source of inconsistency in the matrix. A *CR* value of 0 indicate perfect consistency in the PCM.

Step 4: The consistency index (*CI*) was calculated using Equation (5):

$$CI = \frac{\lambda_{max} - n}{n - 1} \quad (5)$$

Where: λ_{max} is the principal eigenvalue, and n represents the number of parameters selected for the study.

2.4 Weighed overlay analysis

Weigh overlay analysis (WOA) is a simulation method used to generate a composite map by combining the geometry and attributes of various thematic layers within a GIS environment (Mussa et al. 2020). Based on the MCDA concept, WOA enables the blending of multiple raster layers to produce a final result. The goal of WOA is to create a cumulative possibility model that reflects the potential groundwater regions in a given location based on the selected parameters and their respective weights. In this study, WOA is employed to construct the final groundwater distribution potential map.

All specified attributes are converted into raster format and standardized to a uniform cell size within GIS software to identify potential groundwater zones. WOA is regarded as an effective technique for delineating probable groundwater areas, as several recent studies has employed the WOA in GIS platform to assess groundwater potential (e.g. Andualem and Demeke, 2019; Arulbalaji et al. 2019; Abijith et al. 2020; Mussa et al. 2020). The WOA can be expressed using the following Equation (6) (Saranya et al. 2020):

$$WOA = \sum_{i=1}^{n} W_i * R_i \quad (6)$$

Where: W_i is a specific decision criterion, R_i is the raster layer corresponding to that particular criteria, and n is the number of the decision matrices.

2.5 Modeling groundwater potential zone

The potential groundwater zones in the Kulfo-Hare catchment were determined by overlaying various thematic layers that contribute to groundwater potential using GIS and AHP methodologies. The groundwater potential index (GWPI) is a dimensionless metric used to model the prospective groundwater within a region. The weighted integration technique is employed to designate possible groundwater areas using Equation (7) (Hadi et al. 2020; Bhattacharya et al. 2020).

$$\text{GWPI} = \sum_{W=1}^{m}\sum_{j=1}^{n} \text{N}W_j * X_i \tag{7}$$

Where: W_j is the normalized weight of j^{th} thematic layer, X_i is the rank associated with the classes of i^{th} thematic layer, m is the number of total thematic layers used, and n is the total classes of thematic layers.

3 Results and discussion

3.1 Lineament density

Areas in lineament convergence zones are recognized as suitable locations for groundwater storage due to their high infiltration rates and relatively high permeability (Pinto et al. 2017; Murmu et al. 2019; Saranya and Saravanan, 2020). The presence of lineaments promotes increased porosity and permeability, thus a higher lineament density in a region directly corresponds to greater groundwater potential (Ghosh et al. 2020). The lineament density within the Kulfo-Hare catchment can be categorized into five distinct classes. As listed in Table 3, approximately 73.37% of coverage falls with the moderate to very high appropriateness range. This suggests that a significant portion of the research region exhibits a substantial lineament density, which correlates with increased groundwater recharge and high porosity in the areas designated as superior groundwater zones (Fig. 4).

3.2 Land use/land cover

Based on the developed LULC map, the predominant land uses in the Kulfo-Hare watershed encompass cultivated agricultural land, shrubland, natural forest, urban, and water bodies. The study catchment area is characterized by 78.29%, coverage of agriculture-cultivated land, 3.32%, water bodies, 16.93% shrubland, 2.71% natural forest, and 0.25% urban areas (Fig. 5 and Table 4). In agricultural terrains, runoff is often lower and infiltration is higher, while infiltration is typically low in urbanized areas. Consequently, water bodies, shrubland, and agricultural land are assigned high rankings due to their continuous recharge potential, whereas urban areas receive low rankings (Fig. 5) due to their diminishing impact on groundwater capacity (Kaliraj et al. 2013). Therefore, the extensive coverage of agriculture cultivation land in the study area indicates a high suitability for groundwater availability.

Table 3 Distribution of Lineament density suitability in the area and percent

No.	Area / km²	Area / km²	Suitability class
1	55.10	8.85	Very low
2	110.72	17.78	Low
3	190.6	30.61	Moderate
4	160.1	25.71	High
5	106.17	17.05	Very high

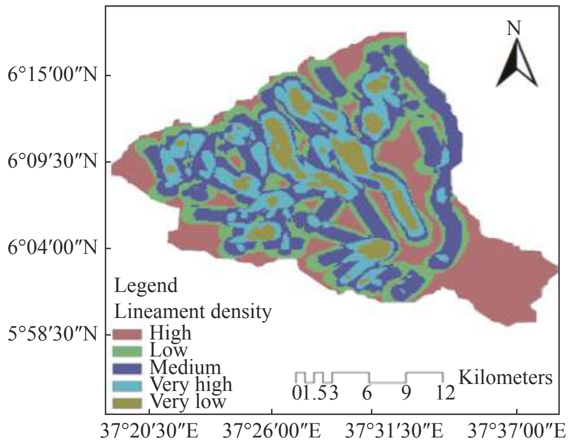

Fig. 4 Lineament density suitability map

3.3 Geological formations

The geological formations of a specific location play a crucial role in determining groundwater availability, as the porosity of different rocks largely influences infiltration and runoff rates (Yeh et al. 2010; Abijith et al. 2020). With the study region, two major geological classes can be identified: Quaternary extrusive and intrusive rocks, and

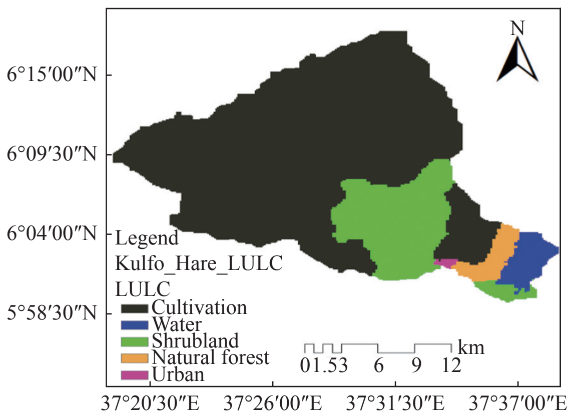

Fig. 5 LULC suitability classification map

Table 4 Distribution of LULC suitability in area and percentage

No.	LULC class	Suitability classification	Area / km^2	Area / %
1	Agriculture cultivation land	Very high	487.51	78.29
2	Water bodies	High	20.68	3.32
3	Shrub land	High	105.45	16.93
4	Natural forest	Moderate	16.86	2.71
5	urban	Very low	1.55	0.25

Tertiary extrusive and intrusive rocks. The geological availability for groundwater potential appears to be relatively uniform across the entire study area (Fig. 6). Both the Quaternary and Tertiary extrusive and intrusive rocks are considered highly favorable areas for groundwater potential. As a result, they are assigned a very high rank as shown in Fig. 6.

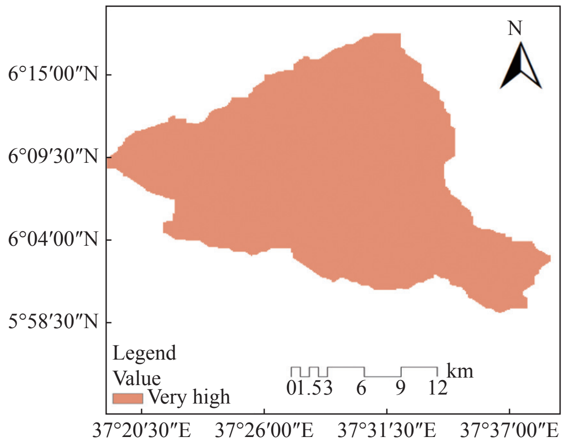

Fig. 6 Study area Geological suitability map

3.4 Slope

The gradient of slope has a direct impact on the rate of rainwater infiltration and is thus used to assess groundwater potential. The steeper the slope tend to result in higher surface runoff and lower groundwater recharge due to limited time for rainwater to percolate the surface. Thus there is an inverse relationship between water infiltration and the degree of slope (Ghosh et al. 2020; Rajasekhar et al. 2019; Murmu et al. 2019). On the other hand, gradual and level slopes provide favorable conditions for groundwater recharge and have promising opportunities for groundwater development. The slopes in the area can be classified into five categories (Fig. 7 and Table 5), with over 50% of total area falling under gentle to moderate slope category. The ranking of these slopes is determined using the groundwater availability data from Table 5.

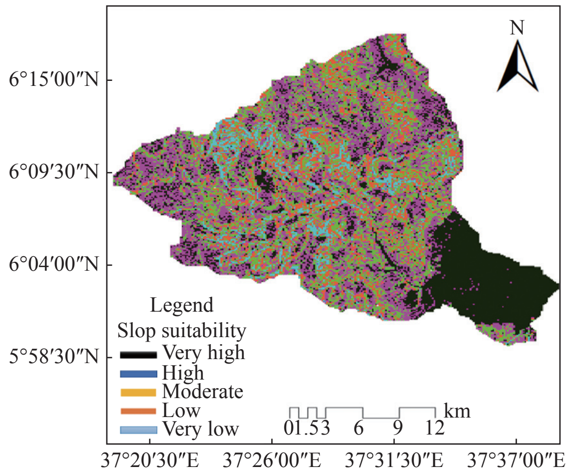

Fig. 7 Slope suitability classification map

3.5 Rainfall

The intensity and duration of rainfall directly influence the rate of groundwater recharge, and in general higher rainfall corresponds to increased infiltration rate and even high groundwater recharge.groundwater capacity renewal, and it aids in

Table 5 Slope suitability distribution in area and percentage

No.	Slope classification	Slope classification	Suitability class	Area / km^2	Area / %
1	<7°	Gentle slope	Very high	151.11	24.4
2	7–15°	Moderate slope	High	191.71	30.8
3	15–24°	Strong slope	Moderate	140.45	23.2
4	24–34°	Steep slope	Low	98.66	16.1
5	>34°	Very steep slope	Very Low	40.76	6.5

the assessment of a balance between subsurface groundwater recharge and discharge (Moges et al. 2019; Datta et al. 2020). Although the Kulfo-Hare area has a high annual rainfall, the annual mean rainfall in current study area is approximately 135.74 mm (Fig. 8). The northern part of the research area experiences the highest annual rainfall compared to the other parts, so that the region receives a very high ranking (Fig. 8). To assess the appropriateness of rainfall for groundwater potential, the study area is classified into five distinct rainfall classes (Table 6).

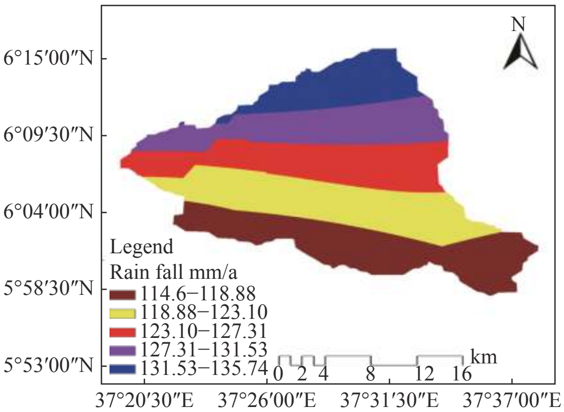

Fig. 8 Rainfall suitability classification map

Table 6 Distribution of rainfall suitability in area and percentage

No.	Rainfall classification / mm	Suitability class	Area / km^2	Area / %
1	114.60–118.88	Very Low	150.33	24.14
2	118.88–123.10	Low	142.31	22.85
3	123.10–127.31	Moderate	130.2	20.91
4	127.31–131.53	High	116.35	18.69
5	131.53–135.74	Very high	83.5	13.41

3.6 Soil

The main soil type in the study area is loam, with sandy loam occurring more commonly towards the south. The loam soil is a very significant soil type that controls groundwater recharge and covers a substantial portion of the research area, particularly in the northern section. According to the generated soil map show in Fig. 9, the loam soil occupies an area of 547.3 km^2 (86.89%), while sandy loam covers an area of 88.41 km^2 (13.11%). The sandy loam and loam soils are considered to have very high and high groundwater potential, respectively (Fig. 9).

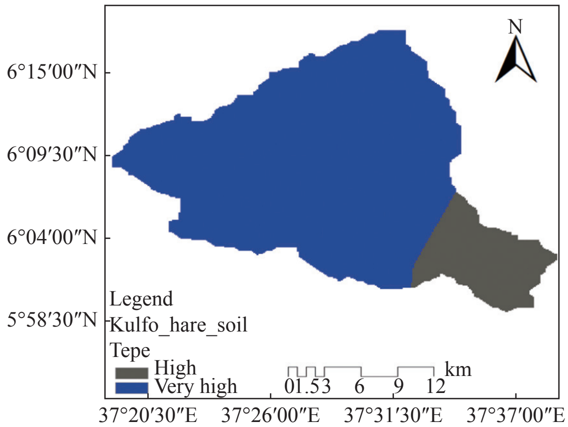

Fig. 9 Soil property suitability classification map

3.7 Drainage density

Drainage density which measures the proximity of channel spacing serves as a permeability indicator (Agarwal and Garg, 2016; Murmu et al. 2019). In terms of groundwater potential, infiltration and permeability are inversely related to drainage density. Higher drainage density indicates limited infiltration, while lower drainage density corresponds to strong infiltration. Therefore, it is regarded as a relatively dominating component in groundwater potential (Patra et al. 2018; Muniraj et al. 2019). As illustrated in Fig. 10 and Table 7, the

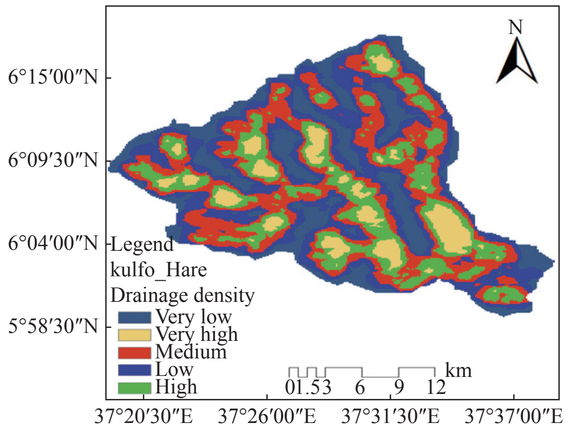

Fig. 10 Drainage density suitability classification map

Table 7 Distribution of drainage density suitability in area and percent

No.	Area / km^2	Area / %	Suitability class
1	127.87	20.54	Very Low
2	120.41	19.34	Low
3	156.38	25.11	Moderate
4	144.95	23.28	High
5	73.08	11.73	Very high

drainage density in the Kulfo-Hare catchment area is classified into five categories based on the suitability of groundwater potential.

The drainage density in the Kulfo-Hare catchment area primarily falls in the moderate to extremely low classes (Table 7), indicating that a significant portion of the study area is favorable for groundwater availability. For the modeling the groundwater potential zones, a low rank is assigned to high density and a high rank to the low density areas (Table 7).

3.8 Weight assigning and normalization of factors using the application of AHP

In this study, the AHP model was applied to derive a pairwise comparison matrix for seven contributing layers (Table 8). The normalized weights for each input factor were determined by calculating the priority vector as shown in Table 9, from which it is evident that geological formation holds the highest weightage of 34%, indicating a input

Table 8 Pairwise comparison matrix of 7 groundwater factors from the AHP model

Factors	LULC	Soil	Geology	RF	Drainage density	Lineament density	Slope
LULC	1	1	3	3	9	9	9
Soil	1	1	3	3	9	7	9
Geology	1/3	1/3	1	1	1	3	3
RF	1/3	1/3	1	1	3	3	3
Drainage density	1/9	1/9	1	1/3	1	1	3
lineament Density	1/9	1/7	1/3	1/3	1	1	3
Slope	1/9	1/9	1/3	1/3	1/3	1/3	1

Table 9 Groundwater potential factors normalized weight using AHP and their sub-classes rank

Factors	Groundwater potential factors classes	Groundwater potential factors suitability	AHP normalized weights	Influence / %	The rank of sub-classes based on Saaty's scale
Lineament density	0–0.2	Very low	0.03	3	1
	0.2–0.4	Low			3
	0.4–0.6	Moderate			5
	0.6–0.8	High			7
	0.8–1.08	Very high			9
LULC	Cultivation land	Very high	0.05	5	9
	Water bodies	High			9
	Shrub land	High			8
	Natural forest	Moderate			5
	Urban	Very low			1
Geology formation	Quaternary extrusive and intrusive rocks	Very high	0.34	34	9
	Tertiary extrusive and intrusive rock	Very high			9
Slope	<7° (Gentle)	Very high	0.1	10	9
	7–15° (Moderate)	High			7
	15–24° (Strong)	Moderate			5
	24–34° (Steep)	Low			3
	>34° (Very steep)	Very Low			1
Annual Rainfall (mm)	114.60–118.88	Very Low	0.32	32	2
	118.88–123.10	Low			4
	123.10–127.31	Moderate			6
	127.31–131.53	High			8
	131.53–135.74	Very high			9
Soil property	Loam	High	0.11	11	9
	Sandy loam	Very high			8
Drainage Density	<1.8	Very low	0.05	5	9
	1.8–2.6	Low			8
	2.6–3.4	Moderate			6
	3.4–4.2	High			4
	>4.2	Very high			2

parameter that influence groundwater recharge. Following closely behind is annual rainfall with a weightage of 32%, and soil property jointly ranks as the third most influencing factor that account for 11% of the overall weightage. Similarly, slope (10%), drainage density (5%), LULC (5%), and lineament density (3%) contribute their respective weightages and positions in determining groundwater potential in the Kulfo-Hare watershed.

To ensure the reliability of determining the weight factors, the consistency ratio (*CR*) was calculated, which was compared to random index values to determine if the matrix weighting was generated randomly. If inconsistencies are found, revisions to the matrix would be necessary to address inconsistent decisions regarding the importance of criteria. However, in this study, the consistency ratio (*CR*) is 0.034, which is lower than the random index values of 1.32 for seven samples. This indicates that the selection of the indicators and their associations is highly relevant in identifying the potential region of groundwater resources in the study area as shown in Table 9.

3.9 Estimation of groundwater potential area

The resulting map (Fig. 10) illustrates the distribution of areas with varying groundwater potential within the Kulfo-Hare region. The high to very high groundwater potential zone covers an area of 244.41 km^2 (39.32%). The moderate groundwater potential zone covers an area of around 152.45 km^2 (24.48%). The low to very low groundwater potential zone comprises around 225.43 km^2 (36.2%) of the study area. According to Fig. 11 and Table 10, a significant portion of the Kulfo-Hare region is covered by high groundwater potential zone. In contrast, the groundwater levels in the remaining parts of the research area are low and constantly inadequate. It is noteworthy that the total area with very high to moderate groundwater potential reaches 396.93 km^2 (63.8%). Thus, it clearly indicates that high groundwater potentiality area dominates the study area.

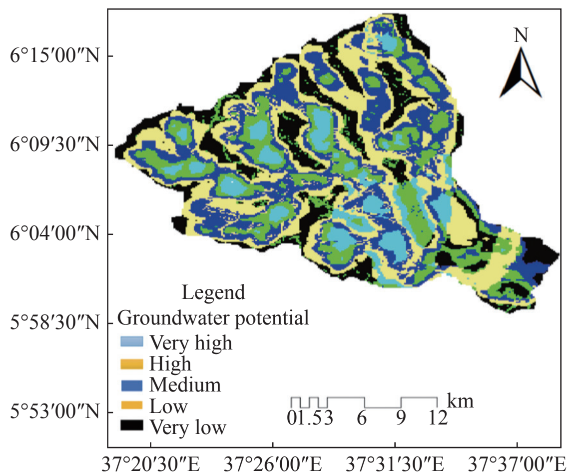

Fig. 11 Groundwater potential distribution map

Table 10 Distribution of groundwater potential area

No.	Suitability area coverage / km^2	Suitability in / %	Groundwater potential distribution class
1	112.92	18.13	Very low
2	112.51	18.07	Low
3	152.45	24.48	Moderate
4	184.12	29.56	High
5	60.36	9.76	Very high

4 Conclusion and recommendation

In this study, seven factors that include LULC, lineament density, slope, geology, rainfall, drainage density, and soil were selected to assess the groundwater potential distribution of the study area located within the Kulfo-Hare catchment. Through the integration of an analytical hierarchy approach, GIS, and remote sensing, the groundwater potential was classified into five categories: Very low (18.13%), low (18.07%), mid (24.48%), high (29.56%), and very high (9.7%). The findings indicate that the majority of the study area (396.93 km^2 or 63.48%) falls within the zone of extremely high to moderate groundwater potential. The remaining area of 225.76 km^2 (36.52%) falls into the low to very-low groundwater potential category, necessitating an urgent groundwater management policy.

The current study, using AHP and GIS techniques, has produced a credible result by utilizing remote sensing satellite data. However, for future research, it is recommended to explore the use of other models such as FR, WOE, MIF, CF, and etc. for delineating the distribution of groundwater potential areas. In addition, encouraging the comparison among various models to assess the accuracy level of with major geographical and hydrological parameters would be beneficial.

References

Abijith D, Saravanan S, Singh L, et al. 2020. GIS-based multi-criteria analysis for identification of potential groundwater recharge zones: A case study from Ponnaniyaru watershed, Tamil Nadu, India. HydroResearch, 3: 1−14. DOI：10.1016/j.hydres.2020.02.002.

Agarwal E, Agarwal R, Garg RD, et al. 2013. Delineation of groundwater potential zone: An AHP/ANP approach. Journal of Earth System Science, 122(3): 887−898. DOI：10.1007/s12040-013-0309-8.

Agarwal R, Garg PK. 2016. Remote sensing and GIS-based groundwater potential and recharge zones mapping using multi-criteria decision-making technique. Water Resource Managment, 30(1): 243−260. DOI：10.1007/s11269-015-1159-8.

Andualem TG, Demeke GG. 2019. Groundwater potential assessment using GIS and remote sensing: A case study of Guna tana landscape, upper blue Nile Basin, Ethiopia. Journal of Hydrology: Regional Studies, 24: 100610. DOI：10.1016/j.ejrh.2019.100610.

Arefin R. 2020. Groundwater potential zone identification at PlioPleistocene elevated tract, Bangladesh: AHP-GIS and remote sensing approach. Groundwater for Sustainable Development, 10: 100340. DOI：10.1016/j.gsd.2020.100340.

Arulbalaji P, Padmalal D, Sreelash K. 2019. GIS and AHP techniques based delineation of groundwater potential zones: A case study from southern Western Ghats, India. Scientific Reports, 9(1): 2082. DOI：10.1038/s41598-019-38567-x.

Ashebir WY, Marc C, Girma K, et al. 2018. Land use and land cover changes and their effects on the landscape of Abaya-Chamo Basin, Southern Ethiopia. Land, 7(1): 2. DOI：10.3390/land7010002.

Bashe BB. 2017. Groundwater potential mapping using remote sensing and GIS in Rift Valley Lakes Basin, Weito Sub Basin, Ethiopia. International Journal of Scientific and Engineering Research, 8(2): 43−50.

Benjmel K, Amraoui F, Boutaleb S, et al. 2020. Mapping of groundwater potential zones in crystalline terrain using remote sensing, GIS techniques, and multicriteria data analysis (case of the Ighrem region, Western Anti-Atlas, Morocco). Water, 12(2): 471. DOI：10.3390/w12020471.

Bhattacharya R, Chatterjee ND, Das K. 2020. An integrated GIS approach to analyze the impact of land use change and land cover alteration on groundwater potential level: A study in Kangsabati Basin, India. Groundwater Sustain Development, 11: 100399. DOI：10.1016/j.gsd.2020.100399.

Biswas Arkoprovo, Jana Adarsa, Mandal Animesh. 2013. Application of remote sensing, GIS, and MIF technique for elucidation of groundwater potential zones from a part of Orissa coastal tract, Eastern India. Research Journal of Recent Sciences, 2(11): 42−49.

Chenini I, Mammou AB, May ME. 2010. Groundwater recharge zone mapping using GIS based multi-criteria analysis: A case study in Central Tunisia (Maknassy Basin). Water Resource Management, 24(5): 921−939. DOI：10.1007/s11269-009-9479-1.

Corti G, Sani F, Philippon M, et al. 2013. Quaternary volcano-tectonic activity in the Soddo region, western margin of the southern Main Ethiopian Rift. Tectonics, 32(4): 861−879. DOI：10.1002/tect.20052.

Das N, Mukhopadhyay S. 2018. Application of multi-criteria decision-making technique for the assessment of groundwater potential zones: A study on Birbhum district, West Bengal, India. Environmental Development Sustainability, 22(2): 931−955. DOI：10.1007/s10668-018-0227-7.

Datta A, Gaikwad H, Kadam A, et al. 2020. Evaluation of groundwater prolific zones in the unconfined basaltic aquifers of Western India using geospatial modeling and MIF technique. Modeling Earth Systems and Environment, 6(3): 1807−1821. DOI：10.1007/s40808-020-00791-0.

Ebinger CJ, Yemane T, WoldeGabriel G, et al. 1993. Late Eocene–Recent volcanism and faulting in the southern Main Ethiopian Rift. Journal of the Geological Society, 150(1): 99−108. DOI：10.1144/gsjgs.150.1.0099.

Elewa HH, Qaddah AA. 2010. Groundwater potentiality mapping in the Sinai Peninsula, Egypt, using remote sensing and GIS-watershed-based modeling. Hydrogeology Journal, 19: 613−628. DOI：10.1007/s10040-011-0703-8.

FAO. 1998. The soil and terrain database for northeastern Africa. Crop production system zones of the IGAD [Intergovernmental Authority on Development] subregion. Rome (Italy): FAO Land and Water Digital Media Series.

Ghosh A, Mandal M, Banerjee M, et al. 2020. Impact of hydro-geological environment on availability of groundwater using analytical hierarchy process (AHP) and geospatial techniques: A study from the upper Kangsabati river basin. Groundwater for Sustainable Development, 11: 100419. DOI：10.1016/j.gsd.2020.100419.

Gintamo TT. 2014. Groundwater potential evaluation. American Scientific Research Journal for Engineering, Technology, and Sciences (ASRJETS), 10(1): 85–120.

Hadi A, Christian O, Suman P. 2021. Identification of groundwater potential zones using remote sensing and GIS techniques: A case study of the Shatt Al-arab Basin. Remote Sensing, 13(1): 112. DOI：10.3390/rs13010112.

Holden J. 2014. Water resources: An integrated approach. New York: Routledge.

Hussein AA, Govindu V, Nigusse AGM. 2017. Evaluation of groundwater potential using geospatial techniques. Applied Water Science, 7(5): 2447−2461. DOI：10.1007/s13201-016-0433-0.

Jha MK, Chowdary VM, Chowdhury A. 2010. Groundwater assessment in Salboni Block, West Bengal (India) using remote sensing, geographical information system, and multi-criteria decision analysis techniques. Hydrogeology Journal, 18(7): 1713−1728. DOI：10.1007/s10040-010-0631-z.

Kaliraj S, Chandrasekar N, Magesh NS. 2013. Identification of potential groundwater recharge zones in Vaigai upper basin, Tamil Nadu, using GIS-based analytical hierarchical process (AHP) technique. Arabian Journal of Geosciences, 7(4): 1385−1401. DOI：10.1007/s12517-013-0849-x.

Machiwal D, Jha MK, Mal BC. 2011. Assessment of groundwater potential in a semi-arid region of India using remote sensing, GIS, and MCDM techniques. Water Resource Management, 25: 1359−1386. DOI：10.1007/s11269-010-9749-y.

Magesh NS, Chandrasekar N, Soundranayagam JP. 2012. Delineation of groundwater potential zones in Theni district, Tamil Nadu, using remote sensing, GIS and MIF techniques. Geoscience Frontiers, 3(2): 189−196. DOI：10.1016/j.gsf.2011.10.007.

Moges DM, Bhat HG, Thrivikramji KP. 2019. Investigation of groundwater resources in highland Ethiopia using geospatial technology. Modeling Earth Systems and Environment, 5(4): 1333−1345. DOI：10.1007/s40808-019-00603-0.

Mukherjee P, Singh CK, Mukherjee S. 2012. Delineation of groundwater potential zone in aridregion of India a remote sensing and GIS approach. Water Resource Management, 26: 2643−2672. DOI：10.1007/s11269-012-0038-9.

Muniraj K, Jesudhas CJ , Chinnasamy. 2019. A delineation of the groundwater potential zone in Tirunelveli Taluk, South Tamil Nadu, India, using remote sensing, geographical information system (GIS), and analytic hierarchy process (AHP) techniques. Proceedings of the National Academy of Sciences, India Section A: Physical Sciences, 90(4): 661−676. DOI：10.1007/s40010-019-00608-5.

Muralitharan J, Palanivel K. 2015. Groundwater targeting using remote sensing, geographical information system, and analytical hierarchy process method in hard rock aquifer system, Karur district, Tamil Nadu, India. Earth Science Informatics, 8(4): 827−842. DOI：10.1007/s12145-015-0213-7.

Murmu P, Kumar M, Lal D, et al. 2019. Delineation of groundwater potential zones using geospatial techniques and analytical hierarchy process in Dumka district, Jharkhand, India. Groundwater Sustainable Development, 9: 100239. DOI：10.1016/j.gsd.2019.10.

Mussa KR, Mjemah IC, Machunda RL. 2020. Open-source software application for hydrogeological delineation of potential groundwater recharge zones in the Singida Semi-Arid, Fractured Aquifer, Central Tanzania. Hydrology, 7(2): 28. DOI：10.3390/hydrology7020028.

Pankaj P, Victor JL, Mahender K, et al. 2020. Application of machine learning techniques in groundwater potential mapping along the west coast of India. GIScience & Remote Sensing, 57(6): 735−752. DOI：10.1080/15481603.

2020.1794104.

Patra S, Mishra P, Mahapatra SC. 2018. Delineation of groundwater potential zone for sustainable development: A case study from Ganga alluvial plain covering Hooghly District of India using remote sensing, geographic information system and analytic hierarchy process. Journal of Cleaner Production, 172: 2485−2502. DOI：10.1016/j.jclepro.2017.11.161.

Pinto D, Shrestha S, Babel MS, et al. 2017. Delineation of groundwater potential zones in the Comoro watershed, Timor Leste using GIS, remote sensing, and analytic hierarchy process (AHP) technique. Appl Water Science, 7: 503−519. DOI：10.1007/s13201-015-0270-6.

Pramanik MK. 2016. Site suitability analysis for agricultural land use of Darjeeling district using AHP and GIS techniques. Modeling Earth Systems and Environment, 2(2): 56. DOI：10.1007/s40808-016-0116-8.

Rahmati O, Nazari Samani A, Mahdavi M, et al. 2015. Groundwater potential mapping at Kurdistan region of Iran using analytic hierarchy process and GIS. Arabian Journal of Geosciences, 8(9): 7059−7071. DOI：10.1007/s12517-014-1668-4.

Rajasekhar M, Sudarsana Raju G, Sreenivasulu Y, et al. 2019. Delineation of groundwater potential zones in the semi-arid region of Jilledubanderu river basin, Anantapur District, Andhra Pradesh, India using fuzzy logic, AHP, and integrated fuzzy-AHP approaches. HydroResearch, 2: 97−108. DOI：10.1016/j.hydres.2019.11.006.

Ramamoorthy P, Rammohan V. 2015. Assessment of groundwater potential zone using remote sensing and GIS in Varahanadhi watershed, Tamilnadu, India. International Journal for Research in Applied Science and Engineering Technology, 3(5): 695−702.

Razandi Y, Pourghasemi HR, Neisani NS. 2015. Application of analytical hierarchy process, frequency ratio, and certainty factor models for groundwater potential mapping using GIS. Earth Science Information, 8(4): 883−886. DOI：10.1007/s12145-015-0220-8.

Saaty TL. 1999. Fundamental of analytic network process. Kobe, Japan: In International Symposium of the Analytic Hierarchy Process (ISAHP) .

Saaty TL, Vargas LG. 2012. Models, Methods, Concepts and Applications of the Analytic Hierarchy Process. New York: Springer Science and Business Media.

Saha S. 2017. Groundwater potential mapping using analytical hierarchical process: A study on Md. Bazar Block of Birbhum District, West Bengal. Spatial Information Research, 25(4): 615−626. DOI：10.1007/s41324-017-0127-1.

Samy IE, Mohamed MM. 2013. Natural hazards susceptibility mapping in the Kuala Lumpur, Malaysia: An assessment using remote sensing and geographic information system (GIS). Geomatics, Natural Hazards and Risk, 4: 1−21. DOI：10.1080/19475705.2012.684725.

Samy IE, Shattri M, Bujang BK, et al. 2012. Application of terrain analysis to the mapping and spatial pattern analysis of subsurface geological fractures of Kuala Lumpur limestone bedrock, Malaysia. International Journal of Remote Sensing, 33(10): 3176−3196. DOI：10.1080/01431161.2011.634860.

Saranya T, Saravanan S. 2020. Groundwater potential zone mapping using analytical hierarchy process (AHP) and GIS for Kancheepuram District, Tamilnadu, India. Modeling Earth Systems and Environment, 6(2): 1105−1122. DOI：10.1007/s40808-020-00744-7.

Sener S, Sener E, Karagüzel R. 2011. Solid waste disposal site selection with GIS and AHP methodology: A case study in SenirkentUluborlu (Isparta) Basin, Turkey. Environmental Monitoring and Assessment, 173(1− 4): 533−554. DOI：10.1007/s10661-010-1403-x.

Shahid S, Nath SK, Roy J. 2010. Groundwater potential modeling in a soft rock area using a GIS. International Journal of Remote Sensing, 21(9): 1919−1924. DOI：10.1080/014311600209823.

Singh LK, Jha MK, Chowdary VM. 2018. Assessing the accuracy of GIS-based Multi-Criteria Decision Analysis approaches for mapping groundwater potential. Ecological Indicators, 91: 24−37. DOI：10.1016/j.ecolind.2018.03.070.

Soumen C, Shyamal D. 2022. Assessment of groundwater potential zone for sustainable water resource management in the southwestern part of Birbhum District, West Bengal. Applied Water Science, 12(3): 40. DOI：10.1007/s13201-021-01549-4.

Thapa R, Gupta S, Guin S, et al. 2017. Assessment of groundwater potential zones using the multi-influencing factor (MIF) and GIS: A case study from Birbhum district, West Bengal. Applied Water Science, 7(7): 4117−4131. DOI：10.1007/s13201-017-0571-z.

Tolche AD. 2020. Groundwater potential mapping using geospatial techniques: A case study of Dhungeta-Ramis sub-basin, Ethiopia. Geology, Ecology, and Landscapes, 5(1): 65−80. DOI：10.1080/24749508.2020.1728882.

Yeh H, Cheng Y, Lin H, et al. 2010. Mapping groundwater recharge potential zone using a GIS approach in Hualian River, Taiwan. Sustainable Environment Research, 26(1): 33−43. DOI：10.1016/j.serj.2015.09.005.